Vol. 15, No. 6, December 2025, pp. 5297~5313

ISSN: 2088-8708, DOI: 10.11591/ijece.v15i6.pp5297-5313

Adaptive tilt acceleration derivative filter control based artificial pancreas for robust glucose regulation in type-I diabetes mellitus patient

Smitta Ranjan Dutta¹, Akshaya Kumar Patra², Alok Kumar Mishra², Ramachandra Agrawal², Dillip Kumar Subudhi³, Lalit Mohan Satapathy¹, Sanjeeb Kumar Kar²

¹Department of Computer Science and Engineering, ITER, S'O'A University, Bhubaneswar, India ²Department of Electrical and Electronics Engineering, ITER, S'O'A University, Bhubaneswar, India ³Department of Computer Science and Information Technology, ITER, S'O'A University, Bhubaneswar, India

Article Info

Article history:

Received Apr 23, 2025 Revised Sep 4, 2025 Accepted Sep 15, 2025

Keywords:

Artificial Controller Glucose Insulin Optimization Pancreas

ABSTRACT

This study proposes an Aquila optimization-based tilt acceleration derivative filter (AO-TADF) controller for robust regulation of blood glucose (BG) levels in patients with type-I diabetes mellitus (TIDM) using an artificial pancreas (AP). The primary objective is to develop a controller that ensures normo-glycemia (70-120 mg/dl) while enhancing stability, accuracy, and robustness under physiological uncertainties and external disturbances. The AO algorithm tunes the control gains of the TADF controller to minimize the integral time absolute error (ITAE), ensuring optimal insulin infusion in real time. The AO-TADF controller introduces a filtered structure to improve the dynamic response and noise rejection capability, effectively handling the nonlinear nature of glucose-insulin dynamics. Simulation results demonstrate that the proposed approach achieves a faster settling time (230 minutes), lower peak overshoot (3.9 mg/dl), and reduced noise (1%) compared to conventional proportional integral derivative (PID), fuzzy, sliding mode (SM), linear quadratic gaussian (LQG), and H∞ controllers. The closed-loop system achieves a stable glucose level of 81 mg/dl under varying meal and exercise disturbances, validating the superior performance and robustness of the AO-TADF approach.

This is an open access article under the <u>CC BY-SA</u> license.



5297

Corresponding Author:

Akshaya Kumar Patra Department of Electrical and Electronics Engineering, ITER, S'O'A University Bhubaneswar 751030, India

Email: akshayapatra@soa.ac.in

NOMENCLATURE

Nomenclature	Description	Nomenclature	Description
$I_p(t)$	Plasma insulin concentration	G(t)	BG level
$I_{abs}(t)$	Insulin absorption rate	Ch	Carbohydrate
V_{I}	Volume of distribution of insulin in deciliter per kg.	Ch_{crit}	Critical value of carbohydrate
$I_a(t)$	Active insulin concentration	$G_{gut}(t)$	Glucose absorption by the gut
K_1	Delay rate of insulin action for I_p	$G_{in}(t)$	Glucose intake rate to the VB from the gut
K_2	Delay rate of insulin action for I_a	K_{gabs}	Glucose absorption rate constant from gut
$I_{ea}(t)$	Effective active insulin	$Tasc_{ge}$	Rising time from 0 to $V \max_{qe}$
$I_{ep}(t)$	Effective plasma insulin	$Tdes_{ge}$	Falling time from $V \max_{ge}$ to 0
s_p	Specific peripheral insulin sensitivity	I_{basal}	Basal value of plasma insulin

Journal homepage: http://ijece.iaescore.com

Nomenclature	Description	Nomenclature	Description
s_h	Specific hepatic insulin sensitivity	$G_{ren}(t)$	Renal excretion of glucose by kidney
$G_{out}(t)$	Total glucose utilization rate for all GM organs.	K_t	Tilt gain
$G_{liver}(t)$	<i>NHGB</i> rate of the liver	K_i	Integral gain
V_G	Glucose distribution volume in the VB	K_d	Derivative gain
n	Coefficient of tilt	N	Pre-filter gains

1. INTRODUCTION

According to the World Health Organization (WHO), one of the most prevalent diseases is diabetes mellitus, which results from pancreatic dysfunction. It lowers insulin sensitivity, which has an impact on a person's blood glucose (BG) level's normo-glycemic range. To cope with this challenge, a number of researchers are currently developing cutting-edge medical devices like a micro insulin dispenser (MID) which is automated. After the open-loop control approach was put into place, the BG concentration was manually maintained. Hypoglycemic or hyperglycemic conditions may arise as a result of difficulties in applying the control loop technique to manage external interruptions and internal system changes. The creation of implanted artificial pancreas (AP) devices that enable the patient's body to get an appropriate dose of insulin based on sensor readings could pave the path for the use of closed loop control techniques. Combination of type-I diabetes mellitus (TIDM) patient model with AP in a closed loop is shown in Figure 1. Three parts constitutes the AP are a MID, a controller, and a sensor. The glucose sensing device monitors the level of blood sugar of the patient model and transfers detailed input to that controller. The control unit delivers a controlling signal using the data from the sensing device. Signal from the controller imparts a signal to the MID for pumping suitable dosage of insulin. To build an optimal solution for the AP, a number of obstacles and limitations must be addressed. These include the influence of non-linear properties, timebased dynamics, various forms of interaction, uncertainties, and an inability to sense glucose.

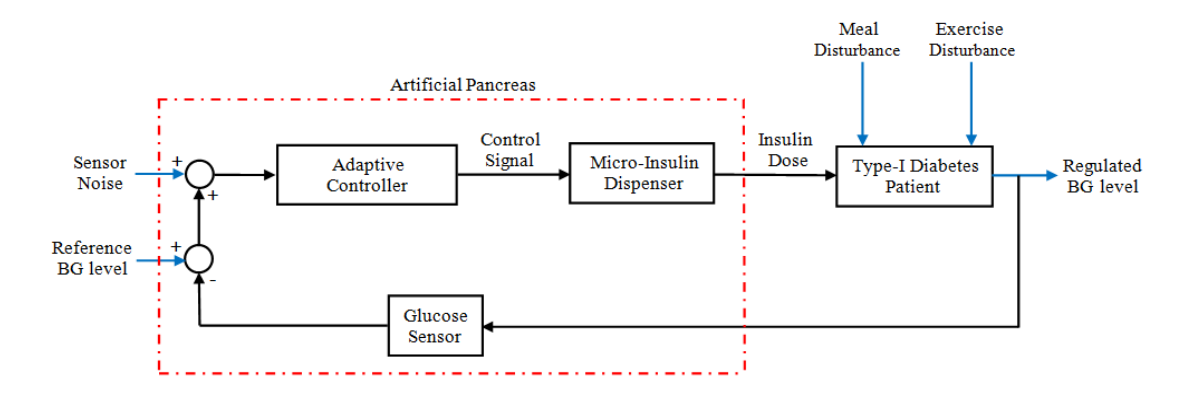


Figure 1. Standard realistic illustration of an AP with TIDM patient

The control challenges include monitoring and assessment of food intake, significant delays in glucose estimation, prolonged insulin uptake after infusion, insulin action generated internally, fluctuations in parameters of the model, risk of extreme BG variations due to its asymmetry, and time-based control requirements [1]-[5]. The aforementioned problem has seen significant technological advancement, but the control algorithm still has to be much improved. The PID controller was suggested by several writers as a workable method for evaluating glucose excursions after AP insulin dosage modifications [6]-[9]. The inability to achieve the necessary performance to provide good robustness, precision, and reliability was caused by non-variable gain factors, insulin action, and the interval between glucose detection. Among the best control strategies to address problems with glucose monitoring are genetic algorithm (GA) [10]-[14], fuzzy [15]–[18], sliding mode (SM) [19]–[22], linear quadratic gaussian (LQG) [23]–[25], H∞ [26]–[28] and model predictive (MP) control [29]-[31]. When patients with normal blood sugar were monitored with the aforementioned controllers, their performance was somewhat enhanced compared to PID controllers. The preceding controllers perform better, but they are not impervious to uncertainty and interruptions in the model. There is no assurance of stability provided by these controllers. They do not have a particularly wide operational frequency range (bandwidth). They do not have as quick control dynamics. Furthermore, they lack complete robustness. In order to prevent slow reaction following a meal disturbance and to enhance performance, the present analysis offers a different innovative method basing on the suggested adaptive controller (AO-TADF). With the use of this AO approach in this proposed method, the controller specifications of AO-TADF are adjusted for better control execution. Following are some justifications for taking into account AO technique:

- AOA exhibits a quicker rate of convergence.

Int J Elec & Comp Eng

- AOA maintains more accurate and consistent outcomes.
- In contrast to other optimization strategies, installation of AOA is simpler and quicker
- AOA increases the algorithm's global and local searching capabilities.
- AOA works with greater accuracy for nonlinear performance indexes like ITAE.

Regarding the aforementioned, the AOA is employed to analyze the value of parameters for control of the recommended controller (AO-TADF) in order to regulate blood sugar in individuals suffering from type I diabetes. This design employs an inventive idea by adding a filter to the TID controller. The filtering process is used to calculate the system states, which are then rapidly drawn towards the point of equilibrium. Consequently, it attains enhanced precision, heightened resilience, superior noise-cancellation effectiveness, and better handling of uncertainty. Secondly, the filtering strategy is used to create a stabilizing control law. Numerous control options are available for system parameters using the recommended controller (AO-TADF). To maintain patient normo-glycemia, the proposed controller adjusts to all potential disruptions and patient circumstances. In contrast to other modern, widely recognized approaches for BG level management of TIDM patients, the suggested approach guarantees a more resilient controller under mismatched and matched uncertainty. The proposed approach introduces a novel AO-TADF controller for robust blood glucose regulation in TIDM patients. The conceptual novelty lies in integrating the AOA to optimally tune the control gains of the TADF controller, ensuring superior noise rejection, robustness, and dynamic adaptability. Unlike traditional methods, AO-TADF handles nonlinearities, uncertainties, and disturbances efficiently, achieving better glycemic control and faster system response under varying physiological conditions. The manuscript's novel contributions include the development of a new AO-TADF controller that integrates AOA with a Tilt Acceleration Derivative Filter to dynamically adjust insulin infusion for TIDM patients. This is the first application of AOA for tuning TADF parameters in artificial pancreas systems, ensuring robustness, precision, and adaptability under physiological uncertainties and meal/activity disturbances. Here is a highlight of the major contributions made by the suggested patient framework with AO-TIDF controller:

- Development of a numerical model to monitor BG levels is based on the patient's glucose metabolism (GM) process.
- To design an AO-TADF controller for a TIDM patient to track BG levels to achieve normo-glycemia.
- Using the AO-TADF controller to examine the patient's features under abnormal circumstances to support its improved performance.
- A comparative analysis is carried out to verify that the recommended technique is superior.

The purpose of this research is to address the challenge of robust BG regulation in TIDM patients, particularly under nonlinear dynamics, uncertainties, and external disturbances, where traditional controllers (PID, LQG, and $H\infty$) fall short in maintaining stable glycemic control. To fill this gap, we propose the AO-TADF controller, which combines AO with a Tilt Acceleration Derivative Filter to enhance adaptability and precision. The main findings demonstrate that AO-TADF achieves faster settling time, reduced overshoot, undershoot, minimal noise, and strong robustness against parameter variations and meal disturbances. These results imply that the proposed controller offers a more effective and reliable control strategy for artificial pancreas systems, improving clinical outcomes for TIDM patients and advancing the design of intelligent insulin delivery systems.

The following is the article's consistent structure: The GM process's possible explanations are displayed in section 2. Section 3 outlines some specifics of the recommended controller's (AO-TADF) method for BG level maintenance. Section 4 shows the simulation and numerical outputs of the AO-TADF controller. Section 5 illustrates the findings from the observations.

2. MATERIALS AND METHOD

Section 2 addresses the clinical background, mathematical model of the non-linear physiological process, and BG profiles of the different organs of the TIDM patient.

2.1. Clinical history

A group of clinical conditions together referred to as diabetes mellitus or hyper-glycemia are characterized by a consistently increasing amount of arterial glucose (AG) exceeding 144 mg/dl. It may be the consequence of insulin activity, insufficiency, or both. The incapacity of the body to utilize glucose correctly is the cause of diabetes. Whether a body is type I or type II depends on the amount of insulin it takes. When a patient has type I diabetes, their body is incapable of producing any insulin at all. In type II

insulin is released more slowly and has a smaller range of action. The body appropriately monitors glucose levels despite the differing demands of meals, fasting, or exercise [32], [33]. That first energy source is glucose. Glucose is required by the human body for every activity. Glucose is taken up and absorbed by the venous blood (VB) from the gastrointestinal tract. Carbohydrate diets deliver glucose into the gastrointestinal region. It is the glucose that is in circulation from an "external" source. The intestine supplies glucose, which the VB then moves to the liver. The liver stores BG as glycogen and while the BG level becomes low enough, it returns to VB. It provides the "internal" glucose. The process of glucose metabolism with oxygen generates energy, carbon dioxide, as well as water inside the cell.

Insulin, which controls BG levels, is produced by the pancreatic β cells. In a normal person with high blood glucose levels, insulin performs two main functions: It first facilitates the liver to take up glucose and transform it into glycogen. which is particularly crucial while consuming meals. Thus, excess "internal" glucose can no longer be produced by the muscles or liver. Secondly, insulin helps the body use glucose in the muscles to meet its peripheral energy requirements. Due to anomalies in the kinetics of metabolic processes, it has been shown that each of these two acts is either completely or partially hindered in diabetic individuals. An uncontrolled blood glucose level is noted in diabetes patients when their cells cease using glucose and the liver generates internal glucose. Kidney function removes extra VB glucose when blood glucose level surpasses 162 mg/dl.

2.2. Structure of the patient

Over the past few generations, glucose-insulin (GI) dynamics demonstrated how the GM process controls glucose, and the authors have offered numerous models to explain this mechanism. Due of its close resemblance to human metabolic processes and structural simplicity, Lehmann *et al.* [32], [33] developed a model which has extensive application in the modelling and testing of various control schemes. During the current investigation, this model has been utilized to evaluate how well the recommended glucose levels to be controlled by the controller. Figure 2(a) shows the six compartments that make up the GM process with AP: the kidney, stomach, liver, brain, and heart.

This model has been employed in the present study to assess the suggested controller's effectiveness in regulating the level of sugar in the blood. Figure 2(a) highlights a six-part structure of the gastrointestinal system's correlation with the assimilated insulin dosage controller: peripheral, kidney, stomach, liver, brain and heart. The liver produces blood glucose, which is then absorbed with the help of the intestinal tract. The AG must be continuously observed in order to provide input to the AP. With the MID placed, the insulin was administered inside the VB is computed in every five minutes, much like the data transmitted to the AP. However, the sample interval is determined by the sensor mechanism and the support mechanism that is used here. This model depicts eating and exercise as unsettling the peripheral and the stomach, respectively. After evaluating insulin, glucose flow, and their attributes, the full GM process in a diabetic patient is synthesized. A simplified model of the TIDM patient's GM process is provided in light of the demonstrated insulin and glucose actions as in Figure 2(b). Solid arrows reflect the transmission of glucose flow patterns. The rise and suppression of blood sugar passage with insulin are shown by 1+ and 1-, correspondingly.

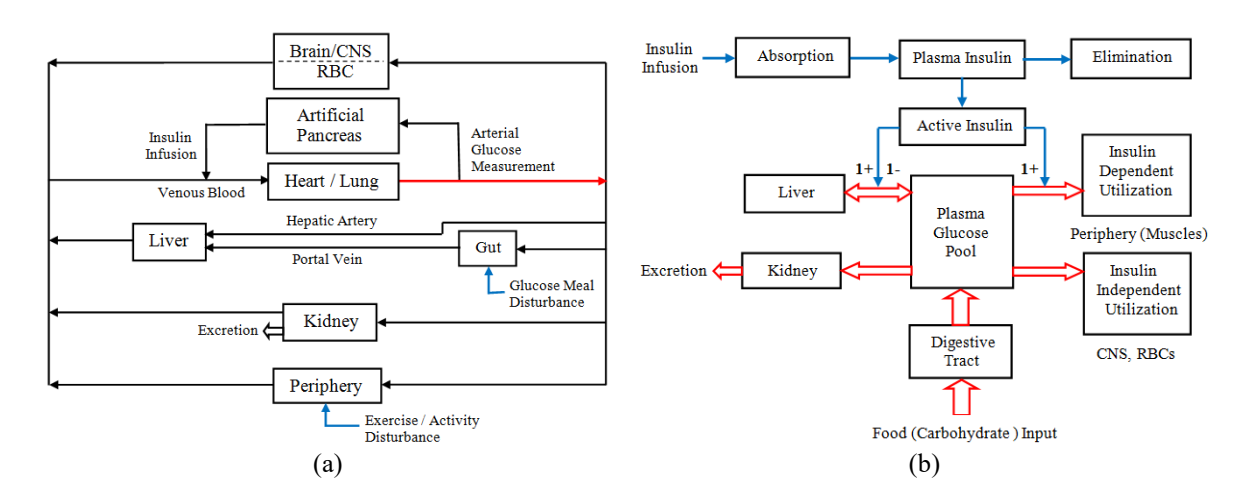


Figure 2. Overall illustration of the GM process in a TIDM patient: (a) compartmental model of the GM system showing the interaction among the kidney, stomach, liver, brain, heart, and peripheral tissues; and (b) simplified representation of the patient structure and the GI dynamics across different body compartments

2.3. Effects of insulin

As the BG level rises, the AP injects the ideal quantity of insulin within the VB stream. The VB's insulin action is described as in reference [32]:

$$\frac{dI_p(t)}{dt} = \frac{I_{abs}(t)}{V_I} - K_e I_p(t) \tag{1}$$

The value of K_e and V_I are assumed as 0.123 min^{-1} and 99.4 dl separately. The differentiation of $I_a(t)$ in the VB is stated as:

$$\frac{dI_a(t)}{dt} = K_1 I_p(t) - K_2 I_a(t) \tag{2}$$

The value of K_1 and K_2 are interpreted as 0.00042 min^{-1} and 0.021 min^{-1} separately. The $I_{ea}(t)$ and $I_{ep}(t)$ within the VB and is mentioned in (3) and (4) accordingly.

$$I_{ea}(t) = S_p(K_2/K_1)I_a(t)$$
(3)

$$I_{ep}(t) = (S_h/I_{basal})I_p(t) \tag{4}$$

The acceptable range for both insulin sensitivity values $(S_p \text{ and } S_h)$ are taken as from 0 to 1.0, and value of I_{basal} is taken as 1.0mU/dl. All insulin action's dynamic conditions during the genetic modification procedures are conveyed in (1) - (4).

2.4. Digestive system's glucose concentration rate

The term "gastric emptying rate" refers to the rate at which the gastric emptying subsystem (GES) forms glucose $G_{empt}(t)$, and presented in the Figures 3(a) and 3(b). $G_{empt}(t)$ attains peak value of $Vmax_{ge}$ (360 mg/min), and eventually drops to 0. The comprehensive plan of $G_{empt}(t)$ plot is contingent upon the quantity of Ch ingestion. Figure 3(a) portrays the triangle shape of $G_{empt}(t)$ under such circumstances of Ch, when the consumption is below the recommended level of Ch_{crit} (10.8 gm). Again Ch_{crit} can be assessed by the help of (5). The $Tasc_{ge}$ and $Tdes_{ge}$ are defined by the (6). Figure 3(b) illustrates a trapezoidal shape of $G_{empt}(t)$ plot in the situation, wheneverCh consumption is same or greater as compared to that of Ch_{crit} , Values of $Tasc_{ge}$ and $Tdes_{ge}$ are reserved as 30 min in this approach. $Tmax_{ge}$ is the period of time during which $G_{empt}(t)$ accomplishes $Vmax_{ge}$. It is referenced in mathematical (7) [32], [33].

$$Ch_{crit} = \left[(Tasc_{ge} + Tdes_{ge})V \, max_{ge} \right] / 2 \tag{5}$$

$$Tasc_{ae} = Tdes_{ae} = Ch/V \max_{ae}$$
 (6)

$$T \max_{ge} = [Ch - (1/2)V \max_{ge} (Tasc_{ge} + Tdes_{ge})]/V \max_{ge}$$
(7)

The $G_{empt}(t)$ with Ch intake higher than Ch_{crit} is categorized as (8):

$$G_{empt}(t) = \begin{cases} (V \max_{ge}/Tasc_{ge})t & if & t < Tasc_{ge} \\ V \max_{ge} & if & Tasc_{ge} < t \leq Tasc_{ge} + T \max_{ge} \\ V \max_{ge} - (V \max_{ge}/Tdes_{ge})t & if & Tasc_{ge} + T \max_{ge} \leq t < Tasc_{ge} + T \max_{ge} + T des_{ge} \\ 0 & if & otherwise \end{cases}$$
(8)

where, t is how much time has passed after a previous meal was taken in. The $G_{empt}(t)$ plots in both triangle and trapezoidal forms are recognized and anticipated for computational purposes as indicated in (8). The 1st order filter production is used to determine the gut's glucose preoccupation rate in relation to the input $G_{empt}(t)$.

$$\frac{dG_{gut}(t)}{dt} = G_{empt}(t) - G_{in}(t) \tag{9}$$

$$G_{in}(t) = K_{gabs}G_{gut}(t) \tag{10}$$

The value of K_{gabs} presumed to be 0.017 min^{-1} . Figure 3(c) shows how quickly the stomach absorbs glucose with 10 and 60gm Ch consumption. It can be achieved by the application of $G_{empt}(t)$ and appears from first order filter depicted in Figures 3(a) and 3(b) distinctly in each of the two situations. Adaptable factors which are listed in (5)-(8) are examined and carried out for the GES. Furthermore, as shown, the dynamic circumstances by (9)-(10) suggested for the stomach are also looked into and as well as employed. The gut's numerical organization is displayed in Figure 4(a).

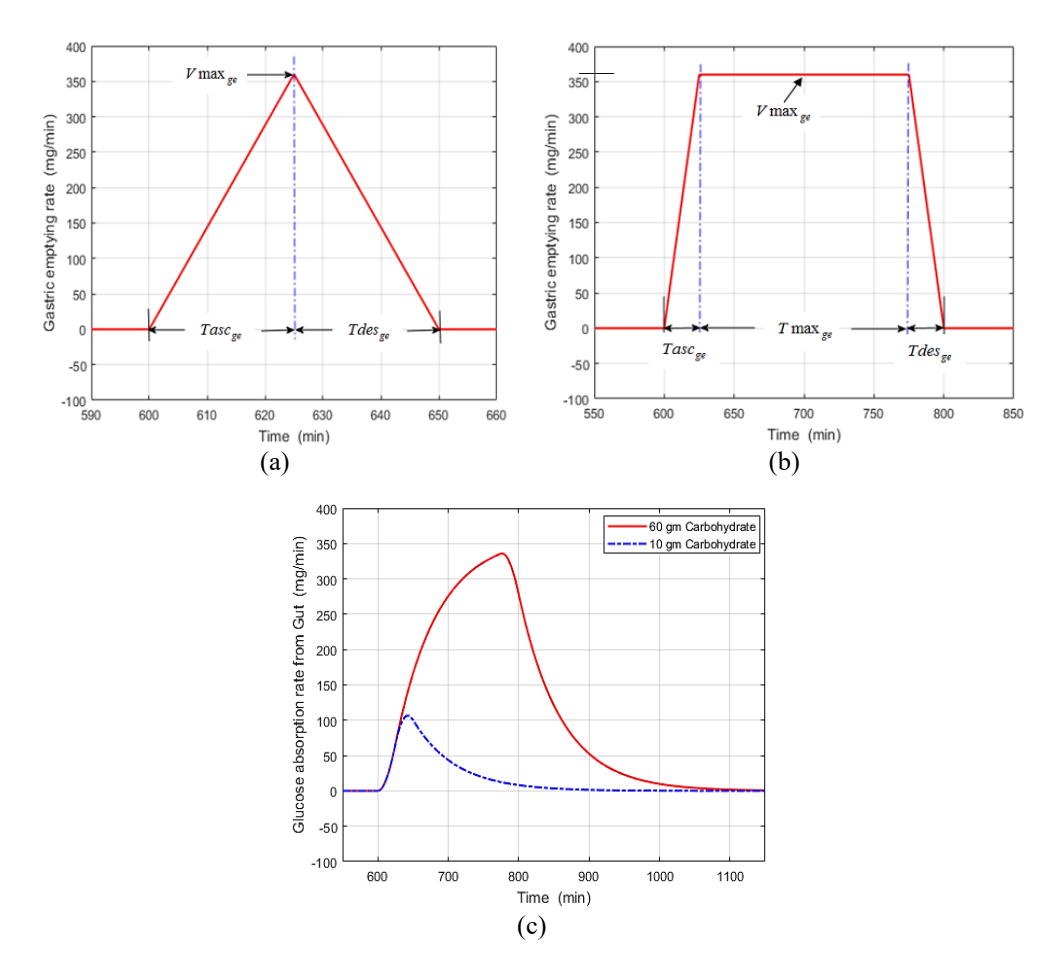


Figure 3. Overall representation of the gastric emptying process and glucose absorption dynamics in response to carbohydrate (Ch) intake in a TIDM patient (a) Plot of $G_{empt}(t)$ with 10 gm Ch absorption ($Ch < Ch_{crit}$) and (b) Plot of $G_{empt}(t)$ with 60 gm Ch absorption ($Ch > Ch_{crit}$); (c) Gut response with 10 and 60 gm Ch absorption

2.5. Glucose profiles in the liver, central nerves system, cells, and red blood cell

Liver is responsible for delivering and using the carbohydrates and is defined as net hepatic glucose balance (NHGB). There are two factors that limit the liver's glucose profile $I_{ep}(t)$ and AG. The look-up table is used to *estimate* it. The relevant data is gathered by taking the literatures for consideration [32], [33]. The liver's computational configuration is replicated in Figure 4(a). Glucose utilization by the cells is dependent on $I_{ea}(t)$ and $I_p(t)$. The lookup table shows how glucose is metabolized by cells, and relevant data is gathered from that literatures. Cell's mathematical structure can be witnessed in Figure 4(a). Red blood cell (RBC) and Brain are the organs that are insulin-autonomous. central nerves system (CNS) and RBC consume carbohydrate of 72 mg/hr/kg and 12.96 mg/hr/kg correspondingly. CNS and renal threshold glucose (RTG) numerical configurations were represented in Figure 4(a).

2.6. Kidney glucose outlines

A portion of the VB's glucose is excreted via the kidney, whenever the BG content G(t) exceeds the RTG. That is denoted as $G_{ren}(t)$. The $G_{ren}(t)$ is dependent on the G(t) and creatinine clearance rate (CCR).

This is expressed logically in (11). $G_{ren}(t)$ decreases to zero, when the value of G(t) is smaller than or identical to RTG as exposed in (12). As per the investigation, CCR and RTG are reserved as 1 dl/min and 160 mg/dl correspondingly. Kidney activity is characterized in accordance to the function [32], [33]:

$$G_{ren}(t) = CCR(G(t) - RTG) \quad if \quad G(t) > RTG$$
 (11)

$$G_{ren}(t) = 0 \quad if \quad G(t) \le RTG$$
 (12)

An illustration of the kidney's analytical organization is shown in Figure 4(a). It is expressed in relation to the terminology used in mathematics as indicated by the (11) and (12).

2.7. VB's blood glucose level

Following is the dynamic expression for the BG level within VB [32], [33]:

$$\frac{dG(t)}{dt} = \frac{[G_{in}(t) + G_{liver}(t) - G_{out}(t) - G_{ren}(t)]}{V_G}$$
(13)

In the present study, V_G is taken as 175 dl. Patient's anatomy is displayed in the Figure 4(a). It is explained according to the mathematical terminology as indicated in (1) - (13).

2.8. Micro insulin dispenser

The references [34]–[37] suggested a specific kind of MID for this investigation. The theory of variable pumping rate governs its operation. The most crucial components of this device are the pump return valve, accumulator, micro pump, storage capsule, and suitable electrical control. Additional sensing and controlling components include an accelerometer to determine whether or not the patient is awake, and a pulse monitor used for measuring the heart rate, and a chromatograph to assess blood glucose levels. A microprocessor compiles all of this data and decides whether to provide the VB with the appropriate dosages of insulin. In Figure 4(b), MID's simulation architecture is displayed.

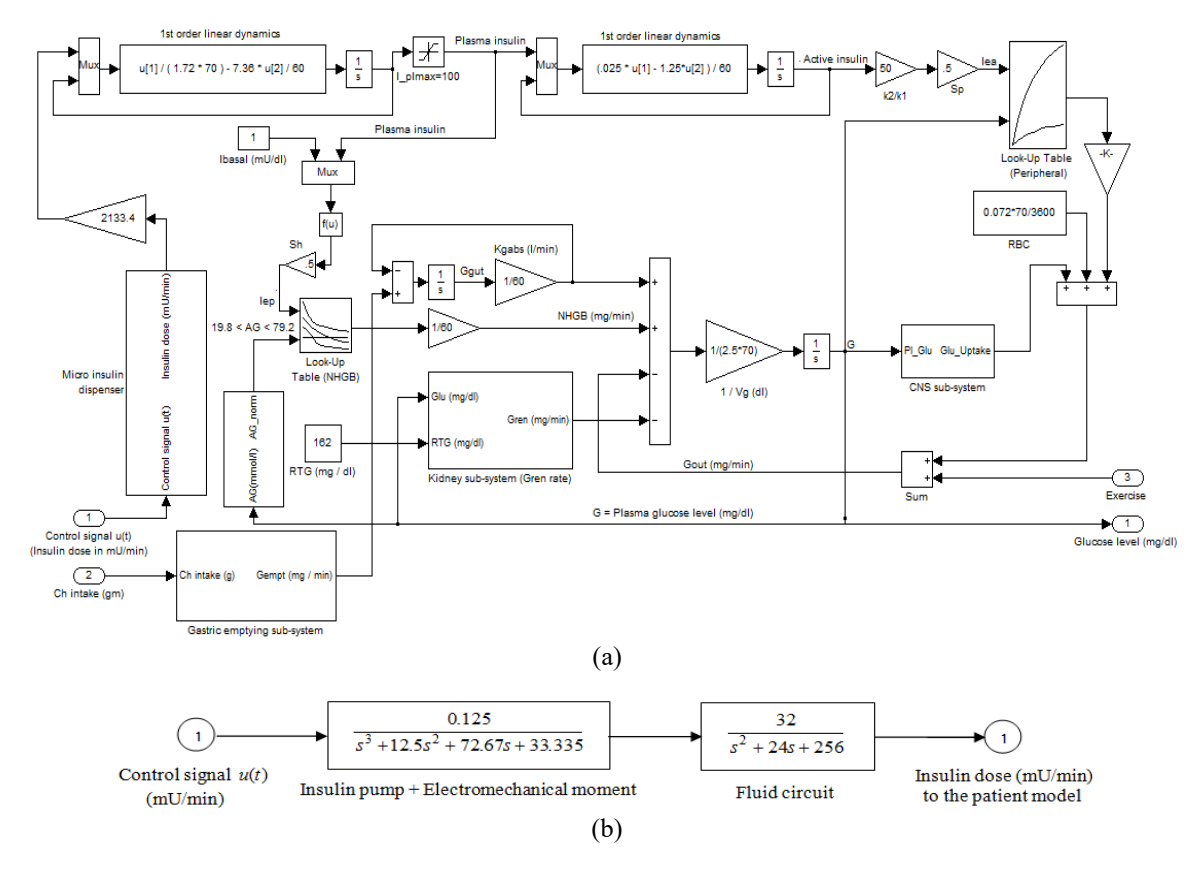


Figure 4. Overall schematic of the AP system and its integration with the TIDM patient model (a) MID simulation framework corresponding to the patient and (b) Simulated structure of MID

2.9. Study of dynamic behavior of the patient

In this section, several variables related to changes in BG metabolic processes during the time-domain responses are illustrated using a 60.00 gm eaten food at 600 minutes and exercising at 1,300 minutes in a Gaussian environment. This study used the insulin dosage that is set fixed, known as the basal insulin dosage. Figure 5(a) shows the insulin dose and brief fluctuations in the plasma glucose concentrations of VB. Figure 5(b) demonstrates anomalies in NHGB rate, gut rate, renal excretion rate and glucose uptake by cells and the CNS.

The liver and peripheral cells in the VB are the only organs that depend on insulin to regulate blood glucose levels. When insulin is absent, they consume comparatively less glucose. Under these conditions, the blood glucose level becomes too high, above the recommended 144 mg/dl. The result is the problem of hyper-glycemia. The kidney eliminates a part of glucose from the VB, when BG level reaches the renal threshold glucose (RTG). The kidney's excretion of glucose in relation to BG levels is shown in Figure 5(c). The implications in Figures 5(a) to 5(c) shows a patient system exhibiting a variety of fleeting responses with the patient's blood glucose levels which consistently exceeds normal values. It illustrates the degree to which the patient's dynamics are susceptible to uncertainty and instability. It is necessary to design an AP using a novel control approach, in order to manage these ambiguities and disturbances in the patient's framework.

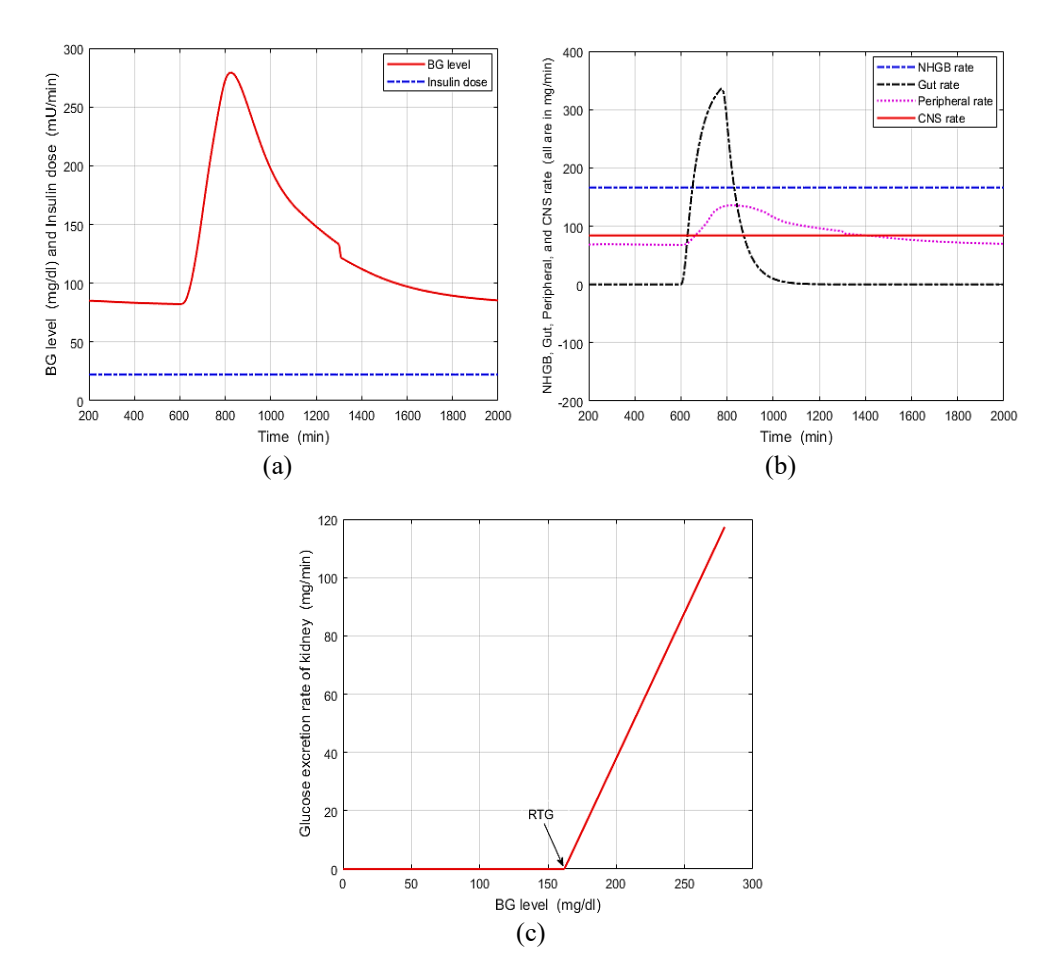


Figure 5. Characteristic curves for the patient model (a) BG level in relation to insulin, (b) rate of glucose synthesis and utilization in GM organs, and (c) rate of glucose excretion by the kidneys

2.10. The mechanisms of control

Addendum subsections clearly establish the AO-TADF control mechanism. Using the AO-TADF controller, the patient's performance is examined for stability, precision, and durability. Indexes of control like settling time t_s (min), steady-state error e_{ss} (%), peak overshoot O_{Peak} , and peak undershoot U_{Peak} are evaluated and the AO-AIDF controller examined closely.

2.10.1. AO-TADF controlling device

Figure 1 depicts the structure of the patient with the AO-TADF controller. Recommended controller's transfer function (TF) is expressed as [38]–[41]:

$$TF = K_t s^n + K_d \left(\frac{N_1 s^\alpha}{N_1 + s^\alpha} \right) + K_d \left(\frac{N_2 s^\gamma}{N_2 + s^\gamma} \right) \left(\frac{N_3 s^\beta}{N_2 + s^\beta} \right) \tag{14}$$

where, the control parameters are represented by tilt gain (K_t) , acceleration gain (K_a) , derivative gain (K_d) , coefficient of tilt (n), pre-filter gains (N_1, N_2, N_3) , coefficient of accelerations $(\gamma \text{ and } \beta)$ and coefficient of derivative (α) . The evaluation of control parameters is based on the response of proposed model for the lowest value of the fitness function (ITAE). Equation (15) highlights the mathematical equivalence of ITAE. The lowest value of fitness function is responsible for better performance such as less overshoot, undershoot, and better monitor glucose levels of proposed model.

$$ITAE = \int_0^\infty |e(t)| t dt \tag{15}$$

The AOA method is used to analyze control parameters for the purpose of monitoring glucose levels.

2.10.2. Optimization technique

The hunting habits of Aquila serve as an inspiration for AO. A potential solution array (X) in AO is created by taking the overall count of candidates (N) and the dimension (D). The dimensions of the array are $N \times D$. Each candidate's selection is determined by [13], [42]–[44] (16).

$$X_{ij} = rand \times (UB_i - LB_i) + LB_i \tag{16}$$

where, X_{ij} , rand, UB_j , and LB_j represents candidate of i^{th} row and j^{th} column in X, an arbitrary value between 0 and 1, Upper limit of j^{th} dimension, lower limit of j^{th} dimension accordingly. Here, i changes from 1 to N, j changes from 1 to D. The hunting technique is usually classified into four stages. These are: i) vertical stooping, high soars, or expanded exploration. ii) short glide or focused investigation during contour flight. iii) reduced flight having brief descent or extended exploitation. iv) walking and catching prey or narrowly focused exploitation.

The aquila soars high to survey the hunting area during the high soar and vertically stooping stages of progression Expanded exploration is the mathematical word for this. This stage is symbolically represented as X_1 . Mathematical expression for the expanded exploration stage is explained in (17).

$$X_1(t+1) = X_{best}(t) \times \left(1 - \frac{t}{T}\right) + \left(X_M(t) - X_{best}(t) \times rand\right)$$
(17)

where, the maximum number of iterations is shown by T, momentary iteration is illustrated by t, the upcoming iteration's resolution is depicted by $X_1(t+1)$, the best option or the location of the prey is exhibited by $X_{best}(t)$ and $X_M(t)$ represents the mean location of the current iteration. In its second phase, the aquila begins hounding and cornering its prey. This stage is referred to as narrowed exploration or contour flying with brief glide. A mathematical expression of the narrowed attempt stage is used to symbolize the narrowed exploration by the (18).

$$X_2(t+1) = X_{hest}(t) \times L(D) + X_R(t) + (y-x) \times rand$$
 (18)

whereas the second mode's answer for the subsequent iteration is $X_2(t+1)$, L(D) indicates the levy propagation for D, $X_R(t)$ signifies the arbitrarily chosen solution for i^{th} iteration, y and x clarifies the Aquila's spiral descent shape. The AO moves into its exploitation stage in the third mode. At this point, the aquila transitions to low flight with either extended exploitation mode or a brief descent state. Aquila watches how prey behaves in this mode of state. This phase is denoted symbolically as X_3 . A mathematical expression for the expanded exploration phase is explained by (19).

$$X_3(t+1) = \alpha \times X_{hest}(t) - \alpha \times X_R(t) - rand + \delta \times rand \times (UB - LB) + \delta \times LB$$
 (19)

whereas, the second mode's answer for the subsequent iteration is $X_3(t+1)$, α and δ depicts the parameters for the exploitation stage adjustment. Aquila mimics its landing in the final mode while bringing down its prey. This stage is characterized as walking and grasping prey, or limited exploitation. This phase is denoted symbolically as X_4 . Mathematical expression for the expanded exploration phase depicted by (20).

$$X_4(t+1) = QF \times X_{best}(t) - G_1 \times X(t) \times rand - G_2 \times L(D) + rand \times G_1$$
 (20)

where, the second mode's provided solution for the subsequent iteration is $X_4(t+1)$, QF represents with the quality function to achieve equilibrium between search approaches, X(t) represents the outcome at i^{th} iteration, G_1 and G_2 illustrates Aquila's motion during the hunting technique. The parameters of the optimization method are set such that the optimum control parameter values are promptly attained. Until to the halt point (maximum iteration), the optimization process continues to be carried out once again. The values of the optimal control parameters are chosen in accordance with the lowest value of ITAE. The optimal controller gains are chosen on the basis of the AOA as mentioned in Table 1. Further TADF's overall architecture is depicted in Figure 6(a), which has been developed on the basis of (14) to (20). An intricate flow chart that illustrates the AOA technique's operation is shown in Figure 6(b). The following 6-steps are required for connection of AOA to the TADF controller:

- a. Initialization: define the search space, including upper and lower bounds for each TADF controller parameter.
- b. Population generation: generate an initial population of candidate solutions randomly.
- c. Fitness evaluation: evaluate each candidate using the ITAE as the performance index.
- d. Optimization phases: apply the four AOA hunting strategies (exploration and exploitation) iteratively to update solutions.
- e. Convergence check: repeat the optimization until the maximum number of iterations is reached or convergence is achieved.
- f. Optimal selection: choose the best candidate solution (with minimum ITAE) as the final set of controller parameters for TADF.

Once the AO-TADF controller is designed, it is integrated with the proposed TIDM patient model, as illustrated in Figure 1. The output response plots of the AO-TADF controller and other compared controllers (such as PID, Fuzzy, SM, LQG, and H ∞) to demonstrate their respective performances. These plots include:

- a. BG level responses under meal and activity disturbances.
- b. Insulin infusion rate profiles.
- c. Comparative visualization of overshoot, undershoot, and settling time for each controller.

Table 1. AO-TADF optimal control parameters

Parameter	Optimal value	Parameter	Optimal value							
K_t (Tilt gain)	0.31	N_2 (Pre-filter gains 2)	9.70							
K_d (Derivative gain)	8.00	N_3 (Pre-filter gains 3)	2.40							
K_a (Acceleration gain)	0.05	α (Coefficient of derivative)	0.63							
n (Coefficient of tilt)	0.06	β (Coefficient of acceleration)	0.31							
N_1 (Pre-filter gains 1)	13.8	γ (Coefficient of acceleration)	0.15							

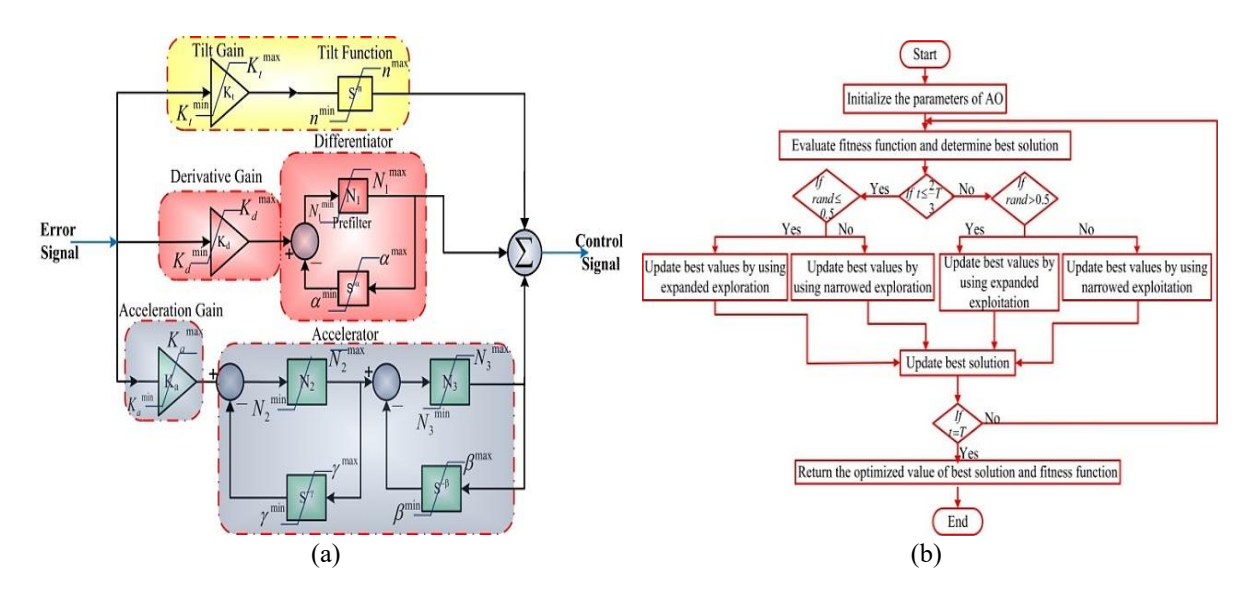


Figure 6. Overall visualization of the AO-TADF control strategy: (a) An AO-TADF block diagram and (b) An AOA flow chart

3. RESULT AND DISCUSSION

The performance of the patient model with AO-TADF in form of accuracy, robustness and stability are fully clarified in the section 4.1, section 4.2, and section 4.3 respectively. Finally, the comparison analysis has been done in detail in the section 4.4.

3.1. Dynamics of the patient under AO-TADF control

The patient model's AO-TADF controller examines every profile and pertinent piece of data that contributes to disturbances and uncertainties, including erratic activity, haphazard glucose intake, noise from sensors and actuators, and so forth. A 60.00 gm meal is consumed at 600 minutes, and 1,300 minutes of exercise are taken to find the characteristic curve that correlates the amount of insulin to blood glucose level as shown in Figure 7(a). Other profiles, including CNS, NHGB, peripheral, gut, and green rates, are represented under the same conditions in Figure 7(b).

The controller's impact from the patient model is seen in Figures 7(a) to 7(c). The liver as well as peripheral cells, which are two insulin-sensitive organs, utilize more glucose as compared to an unregulated process, as the findings clearly demonstrates that in Figures 5(a) to 5(c). This impact causes BG level to drop to 83.3 mg/dl in order to prevent the issue of hyper-glycemia. Now BG level has decreased below the RTG threshold and no additional glucose extraction by the kidney occurs, as predicted in Figure 7(c). Consequently, every patient profile attributes have increased with the usage of AO-TADF controller-based AP.

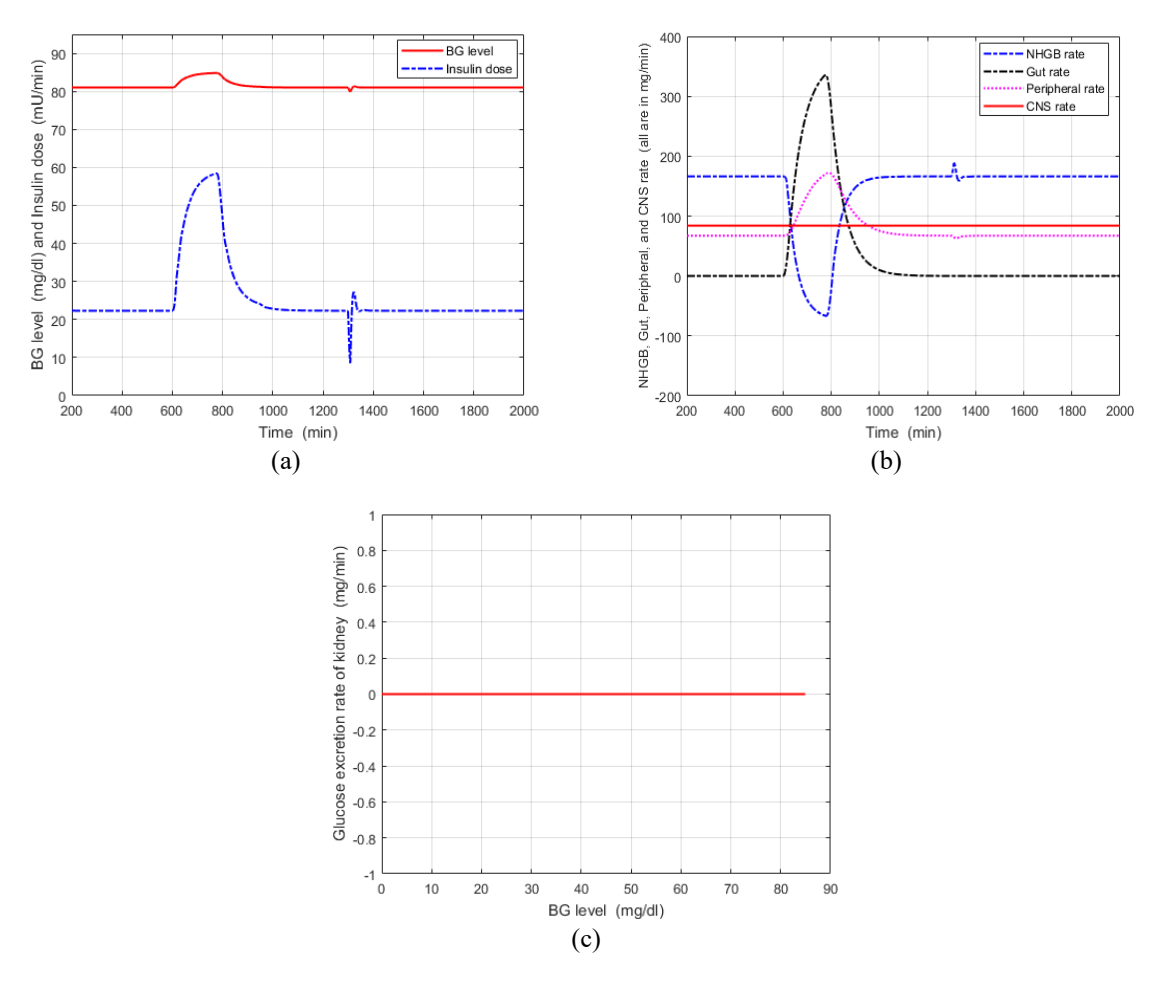


Figure 7. Overall simulation results of the closed-loop TIDM patient model under AO-TADF control (a) Insulin dosage versus BG level, (b) GM organ rates of glucose synthesis and utilization, and (c) BG level versus renal glucose excretion rate

3.2. Robustness features of the AO-TADF controller

It has been established that the suggested controller is resilient against a variety of meal interruptions and two distinct sets of uncertainty regarding the model parameters. Figures 8(a) and 8(b)

exhibit how plasma glucose levels vary right through time with respect to s_h and s_p accordingly. Under various meal disturbance scenarios, the TIDM patient model's BG level change is displayed as in Figure 8(c). The closed loop patient structure exhibits slightly different transient reactions, as seen by the simulation results. But with less settling time, the BG level always reaches 81 mg/dl (normo-glycaemia). As a result, the controller technology used (AO-TADF) is totally impervious to disturbance and model parameter uncertainty. This leads to robustness of a system.

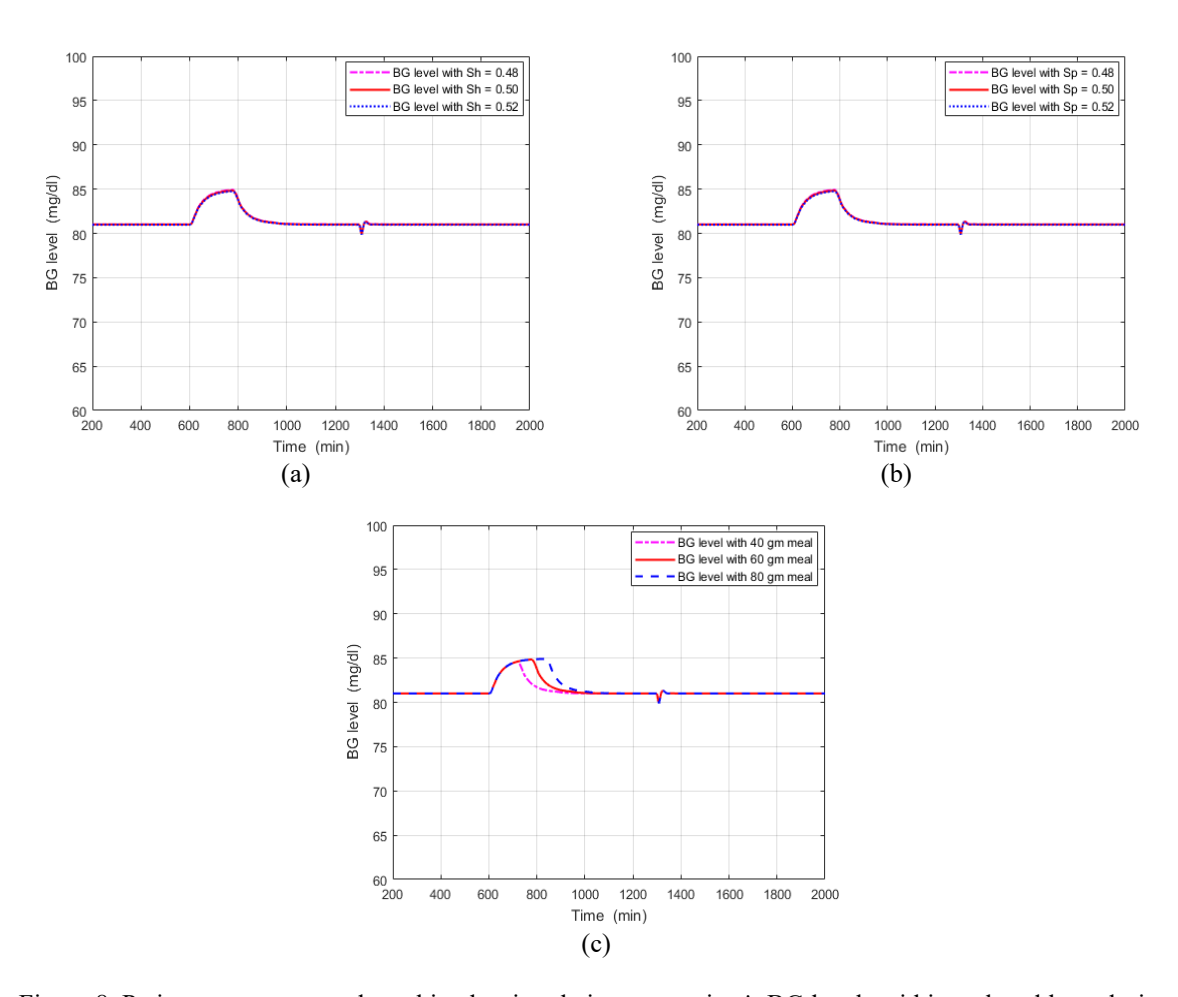


Figure 8. Patient parameters and meal intakes in relation to a patient's BG levels within a closed loop design (a) BG level verses S_p , (b) BG level verses S_p , (c) BG level and meal consumption

3.3. Patient model stability

The bode outputs for both closed and open systems are highlighted in Figure 9 for confirmation regarding requirements for stability that are as follows:

- a. Figure 9(a) represents the open-loop system, which exhibits lower gain and limited bandwidth, indicating weaker control performance and slower system dynamics.
- b. Figure 9(b) (closed-loop with AO-TADF) demonstrates improved gain margin and phase margin, both of which are positive, confirming system stability.
- c. The gain crossover frequency and phase crossover frequency indicate that the system maintains adequate phase lag below -180° at the gain crossover point, ensuring no risk of instability.
- d. Additionally, the wider bandwidth of the closed-loop Bode plot implies faster response and better tracking performance, while the smooth roll-off in magnitude indicates good robustness and damping.

These points collectively confirm the stable and robust performance of the proposed AO-TADF controller.

3.4. Analysis with comparison

The control efficacy of several control methods is compared in this section with the AO-TADF controller. Exercise and skipping meals have an impact on the level of blood glucose and rate of insulin

infusion fluctuations in diabetic patients using this controller. These findings revealed in Figures 7(a)-7(c), and Table 2 conveys certain critical parameters. The chosen controller's overshoot, undershoot, and settling time are somewhat more stable and controllable than other applied optimum controllers, basing on patient BG levels the suggested controller with a 60.00 gm ingested meal disturbance. An activity disturbance test indicates that the BG level regulated by AO-TADF drops to 80.00 mg/dl, which falls inside the range of normal blood glucose. Based on the results, the AO-TADF controller performs significantly more effectively and consistently in lowering noise and solving hyperglycemia concerns. In contrast to other popular controllers, this one lower insulin infusion rates while controlling blood sugar levels. The outcomes demonstrated enhanced robustness, precision, stability, and dependability under various physiological conditions and disturbances by using an AO-TADF based controller.

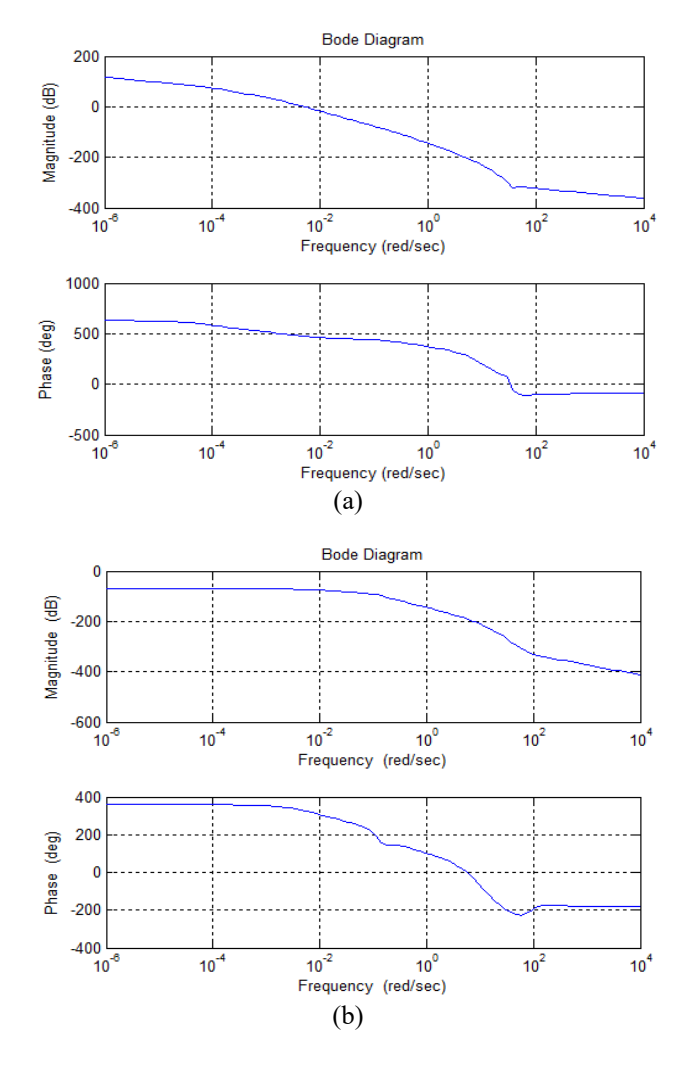


Figure 9. Overall frequency-domain analysis of the TIDM patient model to assess system stability with and without AO-TADF control (a) bode output graphs of the patient structure and (b) AO-TADF regulation and the patient's structure's bode outputs

Table 2. Comparative evaluation using a range of cutting – edge control strategies

PID [4]	Fuzzy [20]	SM [22]	LQG [26]	<i>H</i> ∞ [30]	AO-TADF (Suggested)
60	60	60	60	60	60
58.9	58.8	58.7	58.6	58.5	58.2
285	285	280	270	265	230
5.2	5.3	4.1	8.5	4.5	3.9
3.1	2.1	1.5	1.8	1.2	1.0
10	10	5	5	5	1
0	0	0	0	0	0
	60 58.9 285 5.2 3.1	60 60 58.9 58.8 285 285 5.2 5.3 3.1 2.1	60 60 60 60 58.9 58.8 58.7 285 285 280 5.2 5.3 4.1 3.1 2.1 1.5	60 60 60 60 60 58.9 58.8 58.7 58.6 285 285 280 270 5.2 5.3 4.1 8.5 3.1 2.1 1.5 1.8	60 60 60 60 60 60 58.9 58.8 58.7 58.6 58.5 285 285 280 270 265 5.2 5.3 4.1 8.5 4.5 3.1 2.1 1.5 1.8 1.2

4. CONCLUSION

The new control method (AO-TADF) presented in this study helps TIDM diabetes patients to keep their blood glucose levels within the normo-glycemic range. A thorough mathematical representation and a Simulink model design have been provided for a patient model with MID, in order to facilitate testing and simulation. Every computation was performed using a range of uncertainties and disruptions associated with diet and activity, all of which were based on a typical human operating point. With a base dose of 22.3 mU/min and an operational point determined using a standard human body as a reference with the level of plasma glucose of 81 mg/dl, the investigation was conducted with various uncertainties and disruptions linked to meals and activities of insulin. The recommended control technique is evidently more precise, stable, and robust for regulating the BG level when compared with other control techniques. The consequences suggest that utilizing a fully integrated embedded system in conjunction with extra auxiliary devices and real-time implementation of this type of control mechanism is possible including a MID and a sensor in TIDM patients for BG management. Nevertheless, given the condition of the system at the moment, the technique's associated parameters play a major role in the tuning strategy, which is used to determine the optimal gain. At the same phase and level of the control strategy, this may be prone to vulnerability. Future studies may be carried out to develop a more reliable, strong, and efficient controller for these circumstances, while keeping in mind the aforementioned issues.

The future implications are significant: this approach lays the groundwork for real-time, intelligent insulin delivery systems, and can be extended to other nonlinear biomedical control applications. It also opens avenues for hardware implementation in wearable closed-loop insulin pumps, improving autonomy and safety for diabetic patients.

FUNDING INFORMATION

The authors declare that no funds and grants were received during the preparation of this manuscript.

AUTHOR CONTRIBUTIONS STATEMENT

This journal uses the Contributor Roles Taxonomy (CRediT) to recognize individual author contributions, reduce authorship disputes, and facilitate collaboration.

Name of Author	C	M	So	Va	Fo	I	R	D	0	E	Vi	Su	P	Fu
Smitta Ranjan Dutta	✓			✓					✓		✓		✓	✓
Akshaya Kumar Patra		\checkmark	✓		\checkmark	\checkmark		\checkmark	\checkmark	\checkmark		\checkmark		\checkmark
Alok Kumar Mishra	\checkmark	\checkmark		\checkmark			✓						\checkmark	
Ramachandra Agrawal			✓				✓				✓			
Dillip Kumar Subudhi					✓		✓			✓		\checkmark		
Lalit Mohan Satapathy				\checkmark		\checkmark			\checkmark					
Sanjeeb Kumar Kar	\checkmark		✓					✓		\checkmark		\checkmark		\checkmark

CONFLICT OF INTEREST STATEMENT

Authors state no conflict of interest.

DATA AVAILABILITY

Data availability is not applicable to this paper as no new data were created or analyzed in this study.

REFERENCES

[1] F. Chee, T. Fernando, and P. V. Van Heerden, "Closed-loop glucose control in critically ill patients using continuous glucose monitoring system (CGMS) in real time," *IEEE Transactions on Information Technology in Biomedicine*, vol. 7, no. 1, pp. 43–53, 2003, doi: 10.1109/TITB.2003.808509.

- [2] M. Z. Mohd Tumari, M. A. Ahmad, and M. I. Mohd Rashid, "A fractional order PID tuning tool for automatic voltage regulator using marine predators algorithm," *Energy Reports*, vol. 9, pp. 416–421, 2023, doi: 10.1016/j.egyr.2023.10.044.
- [3] A. K. Patra, N. Nahak, B. Rout, and A. Nanda, "Implantable insulin delivery system based on the genetic algorithm PI controller (GA-PIC)," in *Lecture Notes in Networks and Systems*, 2021, vol. 202 LNNS, pp. 243–252. doi: 10.1007/978-981-16-0695-3 24.
- [4] A. K. Patra and P. K. Rout, "Design of artificial pancreas based on the SMGC and self-tuning PI control in type-I diabetic patient," *International Journal of Biomedical Engineering and Technology*, vol. 32, no. 1, pp. 1–35, 2020, doi: 10.1504/IJBET.2020.104675.
- [5] A. K. Patra, A. Nanda, S. Panigrahi, and A. K. Mishra, "The fractional order pid controller design for bg control in type-i diabetes patient," in *Lecture Notes in Networks and Systems*, 2020, vol. 109, pp. 321–329. doi: 10.1007/978-981-15-2774-6_39.
- [6] A. K. Patra and G. S. Panigrahi, "An adaptive control algorithm for blood glucose regulation in Type-I Diabetes Mellitus patients," *Decision Analytics Journal*, vol. 8, no. 1, pp. 100276–100286, 2023, doi: 10.1016/j.dajour.2023.100276.
- [7] A. K. Patra and A. Nanda, "Design of artificial pancreas based on HGAPSO-FOPID control algorithm," *International Journal of Biomedical Engineering and Technology*, vol. 42, no. 3, pp. 262–280, 2023, doi: 10.1504/IJBET.2023.132546.
- [8] A. K. Patra, G. S. Panigrahi, V. L. Patra, A. K. Mishra, M. K. Debnath, and B. Rout, "Optimal BG regulation in TIDM patient based on adaptive control algorithm," in 2023 IEEE 3rd International Conference on Sustainable Energy and Future Electric Transportation, SeFet 2023, 2023, pp. 1–50. doi: 10.1109/SeFeT57834.2023.10245586.
- [9] S. Mohapatra, A. K. Patra, and D. Rath, "Performance evaluation of grid-connected photovoltaic system using SHO-VPTIDF," Journal of Renewable Energy and Environment, vol. 11, no. 1, pp. 100–121, 2024, doi: 10.30501/jree.2022.355402.1428.
- [10] R. Jadsadaphongphaibool, D. Bi, C. D. Lorenz, Y. Deng, and R. Schober, "Modeling and optimization of insulin injection for type-1 diabetes mellitus management," *IEEE Transactions on Molecular, Biological, and Multi-Scale Communications*, vol. 1, no. 1, pp. 205–214, 2025, doi: 10.1109/TMBMC.2025.3559470.
- [11] D. Rath, A. K. Patra, and S. Kar, "Performance evaluation of grid connected photovoltaic system using AOA tuned VPTIDF," International Journal of Advanced Mechatronic Systems, vol. 10, no. 2, pp. 49–69, 2023, doi: 10.1504/ijamechs.2023.131314.
- [12] A. K. Patra, G. S. Panigrahi, V. L. Patra, A. K. Mishra, N. Nahak, and B. Rout, "Adaptive control with disturbance modelling for BG regulation in TIDM patient," in 2023 International Conference in Advances in Power, Signal, and Information Technology, APSIT 2023, 2023, pp. 583–587. doi: 10.1109/APSIT58554.2023.10201660.
- [13] G. S. Panigrahi, A. K. Patra, A. Nanda, and S. K. Kar, "Adaptive controller design based on grasshopper optimisation technique for BG regulation in TIDM patient," *International Journal of Automation and Control*, vol. 17, no. 4, pp. 440–460, 2023, doi: 10.1504/IJAAC.2023.131773.
- [14] A. K. Patra, G. S. Panigrahi, and A. Nanda, "An automatic artificial pancreas based on AOA-VPTIDF control algorithm," International Journal of Advanced Mechatronic Systems, vol. 10, no. 1, p. 21, 2023, doi: 10.1504/ijamechs.2023.128159.
- [15] A. K. Patra, A. Nanda, B. Rout, D. K. Subudhi, and S. K. Kar, "An automatic insulin infusion system based on the genetic algorithm FOPID control," in *Lecture Notes in Networks and Systems*, 2021, vol. 151, pp. 355–366. doi: 10.1007/978-981-15-8218-9 30.
- [16] A. K. Patra, A. Nanda, B. Rout, and D. K. Subudhi, "Artificial pancreas (AP) based on the JAYA optimized PI controller (JAYA-PIC)," in Smart Innovation, Systems and Technologies, 2023, vol. 317, pp. 11–20. doi: 10.1007/978-981-19-6068-0 2.
- [17] A. Kumar Patra, A. Nanda, and R. Agrawal, "Automated artificial pancreas (AP) based on the JAYA optimized PID controller (JAYA-PIDC)," *Materials Today: Proceedings*, vol. 74, no. 1, pp. 830–835, 2023, doi: 10.1016/j.matpr.2022.11.196.
- [18] A. K. Patra, B. Rout, R. Agrawal, A. K. Mishra, G. S. Panigrahi, and A. Nanda, "An automatic artificial pancreas (AP) based on MO-PID control algorithm," in 2nd Odisha International Conference on Electrical Power Engineering, Communication and Computing Technology, ODICON 2022, 2022, pp. 1–5. doi: 10.1109/ODICON54453.2022.10009980.
- [19] A. K. Patra, A. Nanda, S. Panigrahi, and A. K. Mishra, "Design of artificial pancreas based on fuzzy logic control in type-I diabetes patient," in *Lecture Notes in Electrical Engineering*, 2020, vol. 630, pp. 557–569. doi: 10.1007/978-981-15-2305-2_45.
- [20] A. K. Patra and P. K. Rout, "Backstepping sliding mode Gaussian insulin injection control for blood glucose regulation in type I diabetes patient," *Journal of Dynamic Systems, Measurement and Control, Transactions of the ASME*, vol. 140, no. 9, pp. 91006–91015, 2018, doi: 10.1115/1.4039483.
- [21] A. K. Patra and P. K. Rout, "Adaptive sliding mode Gaussian controller for artificial pancreas in TIDM patient," *Journal of Process Control*, vol. 59, no. 1, pp. 13–27, 2017, doi: 10.1016/j.jprocont.2017.09.005.
- [22] A. K. Patra and P. K. Rout, "An automatic insulin infusion system based on LQG control technique," *International Journal of Biomedical Engineering and Technology*, vol. 17, no. 3, pp. 252–275, 2015, doi: 10.1504/IJBET.2015.068109.
- [23] A. K. Patra, A. Nanda, and P. K. Rout, "Design of backstepping LQG controller for blood glucose regulation in type I diabetes patient," *International Journal of Automation and Control*, vol. 14, no. 4, pp. 445–468, 2020, doi: 10.1504/IJAAC.2020.108276.
- [24] A. Nanda and A. K. Patra, "Kalman filtering linear quadratic regulator for artificial pancreas in type-I diabetes patient," International Journal of Modelling, Identification and Control, vol. 34, no. 1, pp. 59–74, 2020, doi: 10.1504/IJMIC.2020.108916.
- [25] Y. Fang et al., "Metabolic syndrome in type 1 diabetes: higher time above range and glycemic variability revealed by continuous glucose monitoring (CGM)," Diabetology and Metabolic Syndrome, vol. 17, no. 1, p. 49, 2025, doi: 10.1186/s13098-025-01602-1.
- [26] F. Chee, A. V. Savkin, T. L. Fernando, and S. Nahavandi, "Optimal H∞ insulin injection control for blood glucose regulation in diabetic patients," *IEEE Transactions on Biomedical Engineering*, vol. 52, no. 10, pp. 1625–1631, 2005, doi: 10.1109/TBME.2005.855727.
- [27] A. K. Patra and P. K. Rout, "Optimal H

 insulin injection control for blood glucose regulation in IDDM patient using physiological model," *International Journal of Automation and Control*, vol. 8, no. 4, pp. 309–322, 2014, doi: 10.1504/IJAAC.2014.065448.
- [28] A. K. Patra, A. K. Mishra, and P. K. Rout, "Backstepping model predictive controller for blood glucose regulation in type-I diabetes patient," *IETE Journal of Research*, vol. 66, no. 3, pp. 326–340, 2020, doi: 10.1080/03772063.2018.1493404.
- [29] W. Wang, Y. Zhu, G. Zhao, X. Kong, C. Chen, and B. Chen, "A new perspective of blood routine test for the prediction and diagnosis of hyperglycemia," *BMC Endocrine Disorders*, vol. 25, no. 1, p. 115, 2025, doi: 10.1186/s12902-025-01940-1.
 [30] A. K. Patra and A. Nanda, "Model predictive controller design based on the Laguerre functions for blood glucose regulation in
- [30] A. K. Patra and A. Nanda, "Model predictive controller design based on the Laguerre functions for blood glucose regulation in TIDM patient," *Journal of The Institution of Engineers (India): Series B*, vol. 102, no. 2, pp. 237–248, 2021, doi: 10.1007/s40031-021-00549-x.
- [31] A. K. Patra and A. Nanda, "Automated micro insulin dispenser system based on the model predictive control algorithm," International Journal of Advanced Mechatronic Systems, vol. 8, no. 4, pp. 144–154, 2020, doi: 10.1504/IJAMECHS.2020.112629.
- [32] E. D. Lehmann and T. Deutsch, "A physiological model of glucose-insulin interaction in type 1 diabetes mellitus," *Journal of Biomedical Engineering*, vol. 14, no. 3, pp. 235–242, 1992, doi: 10.1016/0141-5425(92)90058-S.

[33] E. D. Lehmann and T. Deutsch, "Compartmental models for glycaemic prediction and decision-support in clinical diabetes care: Promise and reality," Computer Methods and Programs in Biomedicine, vol. 56, no. 2, pp. 193–204, 1998, doi: 10.1016/S0169-2607(98)00025-X.

- [34] L. X. Wang, Design and analysis of fuzzy identifiers of nonlinear dynamic systems, 3rd ed., vol. 40, no. 1. New York: Addison-Wesley, 1995. doi: 10.1109/9.362903.
- [35] A. Kumar Patra, A. Kumar Mishra, G. S. Panigrahi, N. Nahak, V. L. Patra, and A. Nanda, "Artificial pancreas (AP) in diabetes patient based on TLBO algorithm," in 2023 2nd International Conference on Ambient Intelligence in Health Care (ICAIHC), Nov. 2023, pp. 01–05. doi: 10.1109/ICAIHC59020.2023.10431400.
- [36] P. He, Z. ang Chen, Z. Zhou, Z. Liu, and D. Qian, "Robust H2/H∞ DPDC dynamic output feedback controller for an uncertain tensor product model of statically unstable missile," *International Journal of Advanced Mechatronic Systems*, vol. 10, no. 1, p. 33, 2023, doi: 10.1504/IJAMECHS.2023.128164.
- [37] T. Seghiri, S. Ladaci, and S. Haddad, "Fractional order adaptive MRAC controller design for high-accuracy position control of an industrial robot arm," *International Journal of Advanced Mechatronic Systems*, vol. 10, no. 1, p. 8, 2023, doi: 10.1504/IJAMECHS.2023.128155.
- [38] A. K. Patra and A. Nanda, "An automatic insulin infusion system based on kalman filtering model predictive control technique," Journal of Dynamic Systems, Measurement and Control, Transactions of the ASME, vol. 143, no. 2, 2021, doi: 10.1115/1.4048370.
- [39] D. Güneş Kaya et al., "Recurrent education: A promising strategy for enhancing diabetes management and reducing hypoglycemia in children with type 1 diabetes," BMC Endocrine Disorders, vol. 25, no. 1, 2025, doi: 10.1186/s12902-025-01917-0.
- [40] A. Hachana and M. N. Harmas, "Terminal synergetic control for blood glucose regulation in diabetes patients," *Journal of Dynamic Systems, Measurement and Control, Transactions of the ASME*, vol. 140, no. 10, 2018, doi: 10.1115/1.4039716.
- [41] G. S. Panigrahi, A. K. Patra, A. K. Mishra, and S. K. Kar, "Artificial pancreas design for BG regulation in TIDM patient based on sliding mode controller with sliding hyperplane," *International Journal of Advanced Mechatronic Systems*, vol. 11, no. 4, pp. 200–213, 2024, doi: 10.1504/IJAMECHS.2024.143363.
- [42] S. Kar, A. Nanda, A. K. Patra, and G. S. Panigrahi, "Design of artificial pancreas based on adaptive controller with wild goat optimization algorithm," *International Journal of Intelligent Systems Technologies and Applications*, vol. 22, no. 2, 2024, doi: 10.1504/ijista.2024.10061310.
- [43] T. Shuprajhaa, K. Srinivasan, and M. Brindha, "Event triggered constrained regulatory control of blood glucose in type I diabetes mellitus condition," *Automatic Control and Computer Sciences*, vol. 58, no. 3, pp. 289–302, 2024, doi: 10.3103/S0146411624700172.
- [44] L. Abualigah, D. Yousri, M. Abd Elaziz, A. A. Ewees, M. A. A. Al-qaness, and A. H. Gandomi, "Aquila optimizer: a novel meta-heuristic optimization algorithm," *Computers and Industrial Engineering*, vol. 157, 2021, doi: 10.1016/j.cie.2021.107250.

BIOGRAPHIES OF AUTHORS



Smitta Ranjan Dutta 🗓 🖾 🖒 is presently working as research scholar in the Department of Computer Science Engineering, Faculty of Engineering & Technology, Siksha 'O' Anusandhan deemed to be University, Bhubaneswar, India. He has completed his MCA degree from Sriram Engg College Chennai, M. Tech in computer science from Biju Patnaik University of Technology, Bhubaneswar. His research area is artificial intelligence and machine learning. He can be contacted at email: smittaranjandutta@gmail.com.



Akshaya Kumar Patra is is presently working as an associate professor in the Department of Electrical and Electronics Engineering, ITER, Siksha 'O' Anusandhan deemed to be University, Bhubaneswar, India. He received his M. Tech degree from Bengal Engineering and Science University, Shibpur, Howrah, India, in 2006, and Ph.D. degree in biomedical engineering from Siksha 'O' Anusandhan deemed to be University, Bhubaneswar, Odisha, India, in 2018. His main research includes control systems, robust control and biomedical engineering. He can be contacted at email: akshayapatra@soa.ac.in, hiakp@yahoo.com.



Alok Kumar Mishra received the M. Tech degree from IIT Roorkee, India, in 2011 and received the Ph.D. degree from SOA deemed to be University, Bhubaneswar, Odisha, India in 2022. He is currently working as an associate professor with the Department of Electrical and Electronics Engineering, ITER, SOA deemed to be University. His main research interest includes power electronics, drives and control, robust control, power electronics converters, FACTS devices, power quality, and biomedical engineering. He can be contacted at email: alokmishra@soa.ac.in, malok2010@gmail.com.



Ramachandra Agrawal is spresently working as an associate professor in the Department of Electrical Engineering, ITER, Siksha 'O' Anusandhan deemed to be University, Bhubaneswar, India. He received his Ph.D. degree in electrical engineering from Siksha 'O' Anusandhan deemed to be University, Bhubaneswar, Odisha, India, in 2019. His main research includes control systems, robust control, and image processing, biomedical engineering. He can be contacted at email: ramachandraagrawal@soa.ac.in.





Lalit Mohan Satapathy is spresently working as an assistant professor in the Department of Computer Science and Engineering, Faculty of Engineering and Technology, Siksha 'O' Anusandhan deemed to be University, Bhubaneswar, India. He received his M.Tech. degree from Biju Patnaik University of Technology, Orissa, India, in 2009, and Ph.D. degree in signal processing from Utkal University, Bhubaneswar, Odisha, India, in 2024. His main research includes signal processing. He can be contacted at email: lalitsatapathy@soa.ac.in.



Sanjeeb Kumar Kar is presently working as a professor in the Department of Electrical Engineering, Faculty of Engineering and Technology, Siksha 'O' Anusandhan deemed to be University, Bhubaneswar, India. He received his M. Tech and Ph.D. from IIT Kharagpur in control systems, in 2004 and 2011 respectively. His main research includes orthogonal functions, optimal control and different applications of control system in the field of engineering and biomedical technology. He can be contacted at email: sanjeebkar@soa.ac.in.